# Applying Bayesian Inference to Estimate Uncertainties in the Aerodynamic Database of CALLISTO

**Sven Krummen, Pavan Tummala, Jascha Wilken, Etienne Dumont**
**German Aerospace Center (DLR)**
**Institute of Space Systems**
**Robert-Hooke-Str. 7**
**28359 Bremen, Germany**
**sven.krummen@dlr.de; pavan.tummala@dlr.de;**
**jascha.wilken@dlr.de; etienne.dumont@dlr.de**

**Moritz Ertl, Tobias Ecker**
**German Aerospace Center (DLR)**
**Institute of Aerodynamics and Flow Technology**
**Bunsenstraße 10**
**37073 Göttingen, Germany**
**moritz.ertl@dlr.de; tobias.ecker@dlr.de**

**Johannes Riehmer, Josef Klevanski**
**German Aerospace Center (DLR)**
**Institute of Aerodynamics and Flow Technology**
**Linder Höhe**
**51147 Köln, Germany**
**johannes.riehmer@dlr.de; josef.klevanski@dlr.de**

*Abstract*— **The three national space centers DLR, CNES & JAXA have joined their efforts in the project CALLISTO to develop and mature key technologies for future operational Reusable Launch Vehicles (RLVs). The goal of this project is to develop, manufacture and test a reusable Vertical-Takeoff Vertical-Landing (VTVL) first stage demonstrator, which will be operated at the European Spaceport in French Guiana from late 2024.**

**One important aspect in the development of RLVs, but also of aerospace vehicles in general, is the generation of an Aerodynamic Database (AEDB) which characterizes the aerodynamic flying qualities of the vehicle. These databases are commonly aggregated from Computational Fluid Dynamics (CFD) simulations and Wind Tunnel Tests (WTTs) via simple heuristic models. Whereas this classical approach is suitable for the estimation of nominal aerodynamic coefficients, the quantification of uncertainties in this pre-flight data with respect to the final flight behavior is still a difficult task that involves a lot of human expert knowledge and "gut feeling". Particularly for launch vehicles, these uncertainties are however essential to ensure robust guidance and control algorithms, as well as sufficient vehicle performance for a selected mission profile.**

**For CALLISTO, in parallel to a classical approach, a new methodology has now been tested to estimate these uncertainties within the AEDB: To apply Bayesian Inference to predict a probability distribution over the aerodynamic coefficients, conditional on the available test and simulation results and on prior knowledge. This methodology has already been well-established in other data science domains, but for aerospace engineering only very few use-cases are known so far. With this new approach an objectively traceable modelling of the aerodynamic uncertainties should be possible.**

**This paper presents the current development state of the Bayesian aerodynamic uncertainties model of CALLISTO. After problem definition and a short introduction to the underlying dataset, the paper mainly focuses on the used modelling techniques and the applicability of Bayesian methods to the aerodynamic characterization problem. Selected results are shown for Bayesian models and compared against the classical modelling approach, while advantages and disadvantages of the Bayesian methodology are discussed. It is shown that the implemented Bayesian Gaussian process model can infer the typical characteristics of the AEDB from the available datasets, while having comparable prediction qualities as the reference model. Observed differences in the variance and bias characteristics are discussed for both models.**

978-1-6654-9032-0/23/$31.00 

## TABLE OF CONTENTS



## ACRONYMS

| | |
|---|---|
| AEDB | Aerodynamic Database |
| ALS | Approach and Landing System |
| AoA | Angle of Attack |
| AoR | Angle of Roll |
| ATDB | Aerothermodynamic Database |
| CAL1B | CALLISTO Aeroshape Version 1B |
| CAL1C | CALLISTO Aeroshape Version 1C |
| CALLISTO | Cooperative Action Leading to Launcher Innovation for Stage Toss-back Operations |
| CFD | Computational Fluid Dynamics |
| CNES | Centre National d'Études Spatiales |
| CR | Coregion Kernel |
| DLR | Deutsches Zentrum für Luft- und Raumfahrt |
| DNW | German-Dutch Wind Tunnels |
| DoF | Degree of Freedom |
| ELV | Expendable Launch Vehicle |
| ETI | Equal-Tailed Interval |
| FCS/A | Aerodynamic Flight Control System |
| FCS/R | Reaction Flight Control System |
| FCS/V | Vectoring Flight Control System |
| FEM | Finite Element Method |
| FFN | fins folded, legs folded, engine off |
| FFO | fins folded, legs folded, engine on |
| GNC | Guidance, Navigation & Control |
| GP | Gaussian Process |
| HDI | Highest Density Interval |
| HF | High-Fidelity |
| HST | High-Speed Wind Tunnel |
| JAXA | Japan Aerospace Exploration Agency |
| KDE | Kernel Density Estimation |

| | |
|---|---|
| LF | Low-Fidelity |
| LH2 | Liquid Hydrogen |
| LOX | Liquid Oxygen |
| M32 | Matern-3/2 Kernel |
| M52 | Matern-5/2 Kernel |
| MAD | Median Absolute Deviation |
| MCMC | Markov Chain Monte Carlo |
| MVN | Multivariate Normal Distribution |
| PDF | Probability Density Function |
| PDR | Preliminary Design Review |
| RANS | Reynolds-Averaged Navier-Stokes |
| ReFEx | Reusability Flight Experiment |
| RLV | Reusable Launch Vehicle |
| RMSE | Root Mean Squared Error |
| RSR | Reusable Sounding Rocket |
| RTLS | Return-To-Launch-Site |
| SA | Spalart-Allmaras turbulence model |
| SE | Squared-Exponential Kernel |
| TAU | TAU CFD Software |
| TMK | Trisonic Wind Tunnel |
| TVC | Thrust Vector Control |
| UFN | fins unfolded, legs folded, engine off |
| UFO | fins unfolded, legs folded, engine on |
| UUO | fins unfolded, legs unfolded, engine on |
| VI | Variational Inference |
| VTVL | Vertical-Takeoff Vertical-Landing |
| WN | White Noise |
| WTT | Wind Tunnel Test |

## 1. INTRODUCTION

Reusability of launch vehicle stages has been applied with success for several years by SpaceX with the first stage of the Falcon 9 rocket. It appears that this is at least partially the reason for comparatively low launch service costs offered to commercial customers. In order to maintain the competitiveness of launchers in Europe and Japan, Deutsches Zentrum für Luft- und Raumfahrt (DLR), Centre National d'Études Spatiales (CNES) and Japan Aerospace Exploration Agency (JAXA) have decided to collaboratively develop, manufacture, integrate and test a small-scale reusable rocket stage. The three national organizations pursue the following common main goals:

- Develop and mature technologies required for reusable Vertical-Takeoff Vertical-Landing (VTVL) rocket stages,
- Gather know-how, data and lessons learned on the system design of reusable VTVL launcher stages,
- Gather know-how, data and lessons learned on the operation and refurbishment of reusable VTVL launcher stages on an active spaceport.

To achieve these goals the Cooperative Action Leading to Launcher Innovation for Stage Toss-back Operations (CALLISTO) project has been initiated in 2017. Within this collaboration, a Reusable Launch Vehicle (RLV) demonstrator is currently being developed around the already existing LOX-LH2 Reusable Sounding Rocket (RSR) engine from JAXA [1], [2]. This CALLISTO vehicle, as part of the overall CALLISTO system, is designed for maximum performance and therefore particular attention has been put on the mass and aerodynamic characteristics during the development process. In summary, the vehicle mass is less than 4 tons at lift-off, with a diameter of 1.1 m and a length of about 14 m. The aspect ratio is kept similar to operational launch vehicles, which is motivated by aerodynamic performance considerations [3].

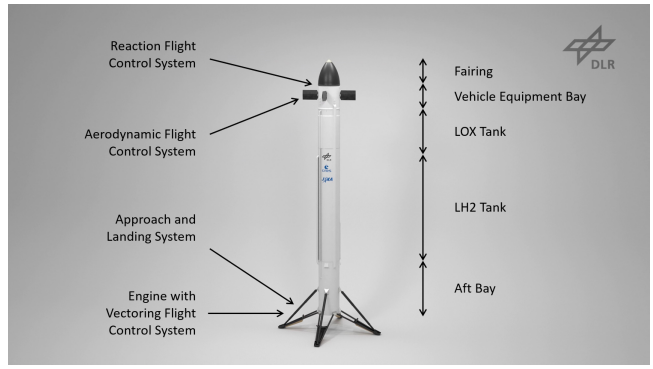


**Figure 1**. Overview of the CALLISTO vehicle; More details are available at [4].

In figure 1 the CALLISTO vehicle is shown with the most important auxiliary subsystems needed for a RLV. The most dominant systems for flight control are:

- Aerodynamic Flight Control System (FCS/A): four actuated and actively controlled aerodynamic fins [5];
- Reaction Flight Control System (FCS/R): based on H2O2 control thrusters;
- Vectoring Flight Control System (FCS/V): based on two actuators for thrust vectoring of the main rocket engine;
- The engine itself, which can be throttled up and down continuously between 40% and 115% of its nominal thrust and be ignited and shut-down during the flight.

Additionally, the CALLISTO vehicle is also equipped with two deployable systems, which are not common on conventional Expendable Launch Vehicles (ELVs) [6]:

- The Approach and Landing System (ALS), with pneumatically deployed legs;
- The Aerodynamic Flight Control System (FCS/A) with electrically deployed fins.

Operations of the vehicle will be performed from the European Space Port in Kourou, targeting the maiden flight in late 2024. Therefore, the former Diamant launch pad, close to the Ariane 5 launch pad, is currently being retrofitted to support the CALLISTO ground segment [7], [8]. It will include a vehicle preparation hall, a launch pad and a landing area. In total, CALLISTO is designed to fly up to 10 times, while an incremental flight test strategy has been defined.

The Preliminary Design Reviews (PDRs) of the systems and of the products are concluded successfully and the consolidation of the design is ongoing, including detailed design, analyses and breadboard testing of the systems and subsystems. An overview and the progress of the project are given in [9], [10], [11], [12].

One important aspect in the development of CALLISTO, but also of RLVs and aerospace vehicles in general, is the generation of an Aerodynamic Database (AEDB) which is essential to characterize the flying qualities of the vehicle. These databases are commonly aggregated from Computational Fluid Dynamics (CFD) simulations and Wind Tunnel Tests (WTTs) via simple empirical-heuristic models. Whereas this classical approach is suitable for the estimation of nominal aerodynamic coefficients, the quantification of uncertainties in this pre-flight data with respect to the final flight behavior is

still a difficult task that involves a lot of human expert knowledge and "gut feeling". Particularly for launch vehicles, these uncertainties are however essential to ensure robust guidance and control algorithms, as well as sufficient vehicle performance for a selected mission profile. On the other hand, the determination of aerodynamic characteristics for RLVs is especially difficult due to the variety of flight control systems and deployable mechanisms onboard, as well as due the complex flight maneuvers like the retro-propulsion phase. Since RLV first stages need to perform a pinpoint landing while carrying only minimal propellant reserves, there was a strong demand during the CALLISTO development process to have a reliable yet not over-constraining estimation of the aerodynamic uncertainties.

For CALLISTO, in parallel to a classical AEDB generation approach, a new methodology has therefore been tested to estimate the uncertainties within the AEDB: Application of Bayesian Inference to predict a probability distribution over the aerodynamic coefficients, conditional on the available test and simulation results and on prior expert knowledge. This methodology has already been well-established in other data science domains such as medicine, astronomy, chemistry, economics and demographics, but for engineering only very few use-cases are published so far. With this new approach an objectively traceable modelling of the aerodynamic uncertainties should be possible, which should incorporate more information from the available datasets and be less effected by subjective expert assessments. Also, such an approach provides the capability to reduce the labor-intense manual investigation of test and simulation datasets, which is necessary during the classical AEDB generation process. Due to this large amount of needed human workforce, classical AEDBs are rarely refitted when new data arrives, whereas for a Bayesian AEDB refitting could be performed in an almost automated manner, requiring computational resources only.

In this paper we want to compare this new Bayesian approach with the classical approach at the example of CALLISTO's AEDB. Here, the central research question that is addressed in the following paragraphs can be posed as: *Is Bayesian inference a suitable method to generate an AEDB with quantified uncertainties for RLVs like CALLISTO?*

After the introduction to the CALLISTO system and the motivation for a Bayesian AEDB in section 1, the available aerodynamic datasets for CALLISTO and their characteristics are described in section 2. The general methodology of Bayesian and classical AEDB generation is explained in 3, together with references to related work. In section 4 this methodology is then applied to some select models for CALLISTO's aerodynamics, followed by some first inference and prediction results in section 5 including a comparison of both models. General discussion and conclusion of the presented material is finally given in section 6, as well as an outlook to future work.

## 2. Dataset Description

The general objective of aerodynamic studies during an advanced vehicle design phase is to create an extensive aerodynamic data set which covers all the relevant flight configurations and conditions. This data set can then be used to generate a database which provides (in the ideal case) continuous data for all dependent variables. Such a database can then be used for 6-DoF flight dynamics simulations. The complexity of both the CALLISTO vehicle shape and

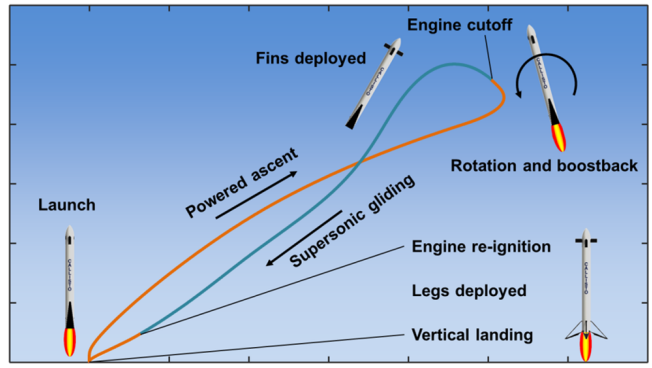


**Figure 2**. Sketch of the typical reference mission profile of CALLISTO.

the number of configurations prohibits the use of classic engineering aerodynamic prediction methods which cannot provide the precision and reliability necessary for the estimation of the aerodynamic coefficients. It is therefore necessary to use advanced CFD methods and WTT experiments to obtain the relevant data [13].

The main objectives during the CALLISTO aerodynamic data generation were:

- Creation of the 6-DoF AEDB containing the aerodynamic function for the calculation of the forces and moments for all configurations.
- Creation of the 6-DoF Aerothermodynamic Database (ATDB) containing the aerothermodynamic function for the calculation of the thermal loads for all configurations (this data is not considered for the current study).

In order to understand the complexity of the CALLISTO flight in terms of aerodynamic configurations, a typical reference mission is visualized in figure 2. After launch the vehicle flies forwards in the ascent phase with active engine and aerodynamic control surfaces folded (FFO configuration). After this powered phase follows a tilt-over maneuver in order to reorient the vehicle for a Return-To-Launch-Site (RTLS) trajectory. The fins are deployed and an aerodynamically controlled gliding phase follows (UFN configuration). At the end of this phase the engines are reignited and a retro-burn maneuver is executed (UFO configuration). During the last stage of this maneuver the legs are unfolded (UUO configuration) and the vehicle touches down. Thus, the aerodynamic data sets of CALLISTO have to be very extensive: Mach number, altitude and dynamic pressure vary in a very broad range, and also Angle of Attack (AoA) and Angle of Roll (AoR) polars need to cover any orientation.

The aerodynamic coefficients and moments are needed for the design of the guidance and control system as well as for the design of vehicle components, such as fins, landing legs or the fairing. Thus, the dependent variables are the following six aerodynamic coefficient and moments which from the core of the AEDB:

- Aerodynamic force coefficients $C_x$, $C_y$, $C_z$,
- Aerodynamic moment coefficients $CM_x$, $CM_y$, $CM_z$.

A wide space of parameters of the flow can influence these aerodynamic coefficients. The following parameters have

| Config | FFO | FFN | UFN | UFO | UUO | UUN | FUFN | FUFO | FUUO | FUO |
|---|---|---|---|---|---|---|---|---|---|---|
| Picture | 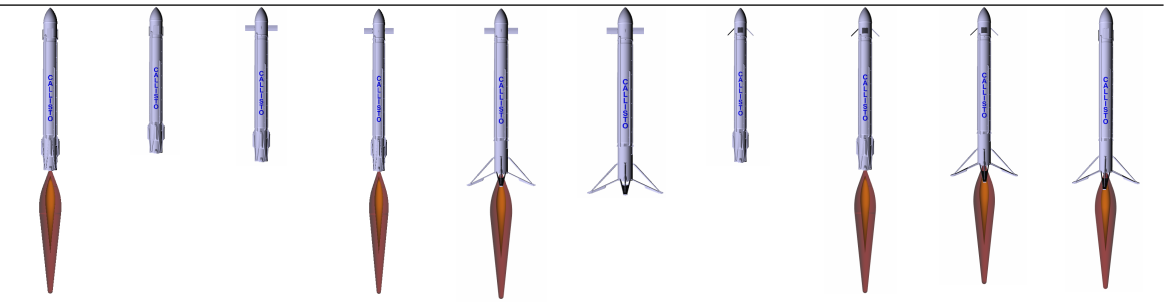 | | | | | | | | | |
| CFD | NS, 2 Gas-Mixture | NS | NS | NS, 2 Gas-Mixture | NS, 2 Gas-Mixture | NS | NS | NS, 2 Gas-Mixture | NS, 2 Gas-Mixture | NS, 2 Gas-Mixture |
| Turbulence Model | SA | SA | SA | SA | SA | SA | SA | SA | SA | SA |
| Roll Range | -180° …+180° | -180° …+180° | -180° …+180° | -180° …+180° | -180° …+180° | -180° …+180° | -180° …+180° | -180° …+180° | -180° …+180° | -180° …+180° |
| AoA Range | 0°…40° | 0°…180° | 0°…180° | 0°…20°, 160°…180° | 0°…180° | 0°…180° | 0°…180° | 0°…180° | 0°…180° | 0°…180° |
| Mach Number Range | 0.5…2.0 | 0.5…2.0 | 0.5…2.0 | 0.5…2.0 | 0.266, 0.5 | 0.266, 0.5 | 0.266, 0.5 | 0.266, 0.5 | 0.266, 0.5 | 0.266, 0.5 |
| Fin Defl. | - | - | -10°,0°,10° | -10°,0°,10° | -10°,0°,10° | 0° | - | - | - | - |
| Fin Depl. | - | - | - | - | - | - | 0°, 45°, 90° | 0°, 45°, 90° | 0°, 45°, 90° | - |
| Leg Depl. | - | - | - | | 20°, 65°, 90°, 115° | 20°, 65°, 90°, 115° | - | - | 115° | 115° |
| Number of LF CFD Sim. | 792 | 2368 | 3312 | 1584 | 1824 | 320 | 1776 | 1776 | 1776 | 592 |
| Number of HF CFD Sim. | 30 | 42 | 262 | 25 | 5 | 1 | - | - | - | 1 |

**Table 1**. Overview of configurations, parameters and number of available CFD data.

been identified as most influential and thus have been chosen as independent variables:

- Mach number $Ma$,
- Altitude $H$, encoding the air density $\rho$ and Reynolds number $Re$,
- Angle of Attack $\alpha$,
- Angle of Roll $\phi$,
- Fin deflection angles $\delta_{j=1..4}$,
- Fin deployment angles $\eta_{j=1..4}$,
- Leg deployment angles $\lambda_{j=1..4}$, and
- Engine thrust level $\tau$.

In addition to the flow parameters the geometric configuration of the vehicle also influences the aerodynamic forces. The different configurations that have been considered are shown in table 1. They are defined by a combination of deployment status of the fins and the landing legs as well as the status of the engine. Additionally, two versions of the aeroshape exist: a preliminary version called CAL1B with a simpler geometry with rotational symmetry; and a more mature version of the aeroshape called CAL1C with higher detail including protrusions from cable ducts and pipes.

In order to establish an extensive aerodynamic dataset for CALLISTO's AEDB, the aeroshape of each configuration has been analyzed with various methods. The generated datasets can roughly be classified in the following categories:

- WTT-sourced data: HST, TMK
- CFD-sourced data: TAU HF, TAU LF
- Semi-empirical data: DATCOM

The following sections will briefly highlight the generation process for each aerodynamic dataset, particularly the simulation setup for CFD data and the experimental configuration for WTT data. Also, typical error characteristics inherent to each method are shortly described.

*Computational Fluid Dynamics*

The numerical simulations are done using the DLR TAU code [14]. TAU is a finite volume computational fluid dynamics code solving the Reynolds-Averaged Navier-Stokes (RANS) equations on hybrid structured-unstructured grids. For the generation of the AEDB the simulations were done with second order temporal and spatial accuracy using a AUSMDV upwinding difference scheme with least-squares gradient reconstruction and an explicit Runge-Kutta scheme. A modification of the variable reconstruction according to Thornber [15] is employed to improve the computation for low Mach numbers together with the one-equation Spalart-Allmaras turbulence model (SA) [16]. For plume modelling a gas mixture representing the exhaust gases and a gas mixture representing air are used with a frozen chemistry assumption.

Two fidelity classes for the mesh size are used to be able to fulfill two requirements: provide a large parameter space and provide a good computational accuracy. The large amount of

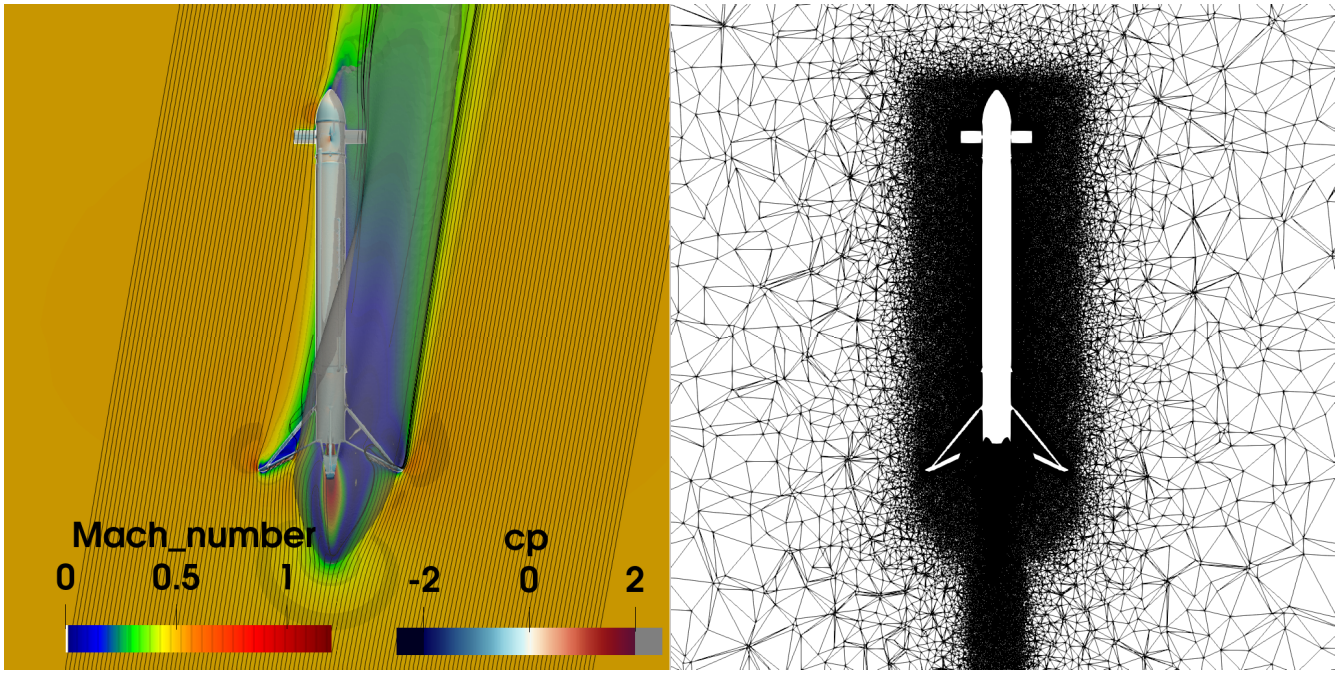


**Figure 3**. Visualization of CFD data for configuration UUO, $Ma = 0.5$, $rho = 1.2\mathrm{kg\,m^{-3}}$ AoA = 170°, AoR = 0°, Thrust level = $100\%$. On the left: Mach number slice with streamlines, plume contour and $c_p$ on the vehicle surface. On the right: visualization of the TAU HF grid.

simulations needed to cover all the above described independent variables necessitates fast simulation times and thus a smaller sized grid. A good accuracy, on the other hand, depends on the grid resolution and thus necessitates a large grid. The underlying AEDB generation logic combining these two fidelity classes is described in detail in the following chapter.

The High-Fidelity (HF) grid comprises 23 million elements and is set up to have a dimensionless wall distance $y^+ < 1.0$ in the first boundary layer cell and 20 prism layers at viscous wall boundary conditions. The Low-Fidelity (LF) grid has 3 million elements and allows for $y^+ \leq 2.0$ in areas of high geometric complexity and has been tailored towards acceptable accuracy under minimal computational costs with the help of HF simulations. The simulations on the HF grid take about 24 hours on 512 cores to reach a converged solution. The simulations on the LF grid take about 20 min on a local workstation, allowing for a far greater amount of parameter variations while keeping the accuracy acceptable. A more detailed explanation of the numerical settings as well as an analysis of the data can be found in [17], [18]. A visualization of an example CFD result is shown in figure 3.

There are various error sources and uncertainties at play when conducting CFD studies. In terms of errors associated with the solver, three recognized sources of numerical errors exist: round-off errors, iterative convergence errors and discretization errors [19]. While some of these errors are controlled by methods within the code design, others are covered by systematic trials and user expert knowledge. The discretization errors are a direct result of the grid generation process. For a simple grid this discretization error is easily calculated from systematic grid convergence studies [20]. For complex geometries these studies are more elaborate as unstructured grids with non-homogenous cell sizes and cell growth rates used to resolve relevant flow phenomena (boundary layer grids, regions with strong shocks and flow gradients) add complexity to systematic mesh refinement. For similar flows we have previously conducted grid convergence index studies and found the discretization errors within the asymptotic range [21].

Further sources of error constitute the physical modelling. As the simulations are done as steady state RANS simulations a major source of error is the turbulence modelling. Furthermore, the steady state doesn't represent unsteady phenomena and also ignores the transient between trajectory points. Another source of errors in the case of simulations with an operational engine is the chemical modelling of the plume. For the presented simulations an assumption of frozen chemistry and two species mixtures representing air and exhaust gases was made due to low presence of unburnt hydrogen at the nozzle exit.

*Wind Tunnel Tests*

Two extensive WTT campaigns have been performed to create and verify CALLISTO's AEDB. A detailed description of these tests for the CAL1C aeroshape in UFN and FFN configuration can be found in [22].

The first test campaign was conducted with a 1:35 model in the Trisonic Wind Tunnel (TMK) of the DLR in Cologne for flow conditions in the range of $Ma = 0.5..2$ and $Re = 0.38..1.11 \times 10^6$. The second campaign was conducted in the High-Speed Wind Tunnel (HST) wind tunnel of the German-Dutch Wind Tunnels (DNW) in Amsterdam with a larger and more detailed 1:10 model, as shown in figure 4. Flow conditions in the range of $Ma = 0.2..1.3$ and $Re = 0.14..4.10 \times 10^6$ have been investigated here.

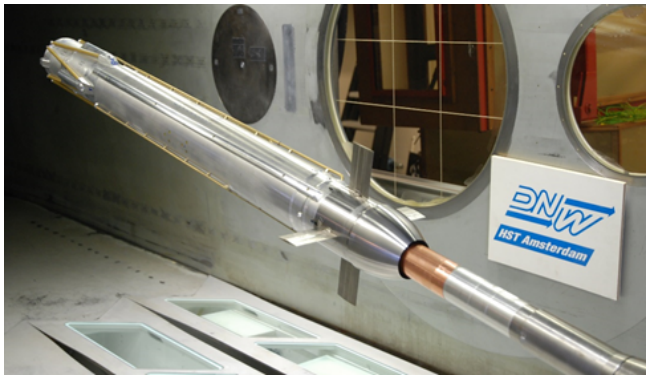


**Figure 4**. UFN wind tunnel model during HST campaign.

In both wind tunnels the aerodynamic forces and moments of the vehicle model have been measured for $\alpha = -10°..10°$ for FFN configuration, respectively $\alpha = 170°..190°$ for UFN configuration, and all $\phi$. Additional pressure measurements and schlieren-imaging was performed but not directly used for AEDB generation.

In total about 118 polars have been recorded during the TMK campaign and about 490 polars during the HST campaign. Due to this huge amount of experimental data, it has been reduced to multiple selected AoAs polars at constant roll angles and Mach numbers in the scope of the analysis presented in this paper.

The main source of uncertainties in the WTT datasets are created from the uncertainties in the measurements of the balance and in determination of the flow conditions. Further systematic uncertainties are originating from the actual experimental setup in the wind tunnel, like sting or wall influences on the vehicle. Compared to the actual CALLISTO vehicle, uncertainties can be also induced by deviations from geometric or dynamic similarities, e.g. due to simplification of the aeroshape for subscale manufacturing or due to differences in the Reynolds numbers between experiment and flight. Since different models have been tested in different wind tunnels with different measurement equipment, the influence of each error contributor should also be different between TMK- and HST-sourced data.

*Semi-Empirical Correlations*

In addition to the aerodynamic datasets generated by CFD simulations and WTT experiments, which form the backbone of CALLISTO's AEDB, some complementary data has been generated from well-known semi-empirical correlations. These correlations have been developed in the past from an extensive range of experiments, in order to estimate aerodynamic coefficients of a vehicle from a simple parametrization of its geometry. Since these correlations require very little computational resources but commonly imply high uncertainty, these results are usually considered during the conceptual design phase only [23]. For CALLISTO these results have therefore only be used for cross-validation, particularly in flight conditions where the other datasets are very sparse.

The dataset for CALLISTO has been generated with the software tool Missile DATCOM [24]. So far, the FFN and UFN configurations have been evaluated for 4736 flight conditions each. This dataset covers the Mach range $Ma = 0.5..2$ for the full AoA and AoR range. Fin deflections have not yet been considered in this dataset. However, due to the short runtime of Missile DATCOM this dataset could easily be extended, if needed. Whereas Missile DATCOM provides also the capabilities to model engine-on configurations, the analysis of vehicle configurations with deployed legs will likely not possible, since such surface features are not foreseen in the geometry parametrization of this software.

Generally, it can be stated that these semi-empirical estimates have often a significant uncertainty in its data. These errors are especially large for complex aeroshapes, like CALLISTO, and for unusual flight conditions, like $\alpha \approx 90°$. This is primarily caused by the fact that tools like Missile DATCOM have a very simple underlying mathematical model, which has been fitted to experimental data from generic aeroshapes for common flight conditions. Compared to before-mentioned CFD- or WTT-sourced data, these estimates can therefore be considered as least reliable for CALLISTO. The qualitative behavior of the aerodynamic coefficients is however often represented adequately by these semi-empirical models.

## 3. METHODOLOGY

The major motivation to create an AEDB is the prediction of aerodynamic coefficients for arbitrary flight conditions which could not explicitly covered by simulations or experiments. For CALLISTO two approaches have been followed to generate such a continuous aerodynamic model from the aerodynamic datasets: a classical AEDB and a Bayesian AEDB. Whereas the classical AEDB employed well-known techniques and therefore serves currently as reference for design and analyses, the Bayesian AEDB experimented with several new approaches to overcome shortcomings in the uncertainty quantification of the classical model. The applied methodologies to generate these AEDBs will be explained in the following paragraphs.

*Formal Definition of AEDB Function*

From a mathematical point of view, the generation of an AEDB function can be seen as a classical curve fitting task to find an appropriate regression function for the collected aerodynamic datasets. As already highlighted in section 2, the outputs of such an AEDB function are the aerodynamic force and moment coefficients which are concatenated for convenience to the coefficient vector $\mathbf{c}$. These coefficients depend on the flow characteristics, the vehicle orientation, the parametrization of the aeroshape, as well as on any error characteristics. Without loss of generality these dependencies can be subsumed to a generalized input vector $\mathbf{x}$. Together with a generalized parameter vector $\boldsymbol{\theta}$, which contains any regression parameters, the AEDB function can be formalized as:

$$\mathbf{c} = f(\mathbf{x}; \boldsymbol{\theta}) \tag{1}$$

With this notation the AEDB generation process, also known as *fitting* or *inference*, can be described as the problem:

$$\begin{aligned} \text{Select} \quad & f, \boldsymbol{\theta} \\ \text{such that} \quad & \tilde{\mathbf{c}}_i \approx f(\tilde{\mathbf{x}}_i; \boldsymbol{\theta}) \\ \text{for all data} \quad & (\tilde{\mathbf{c}}_i, \tilde{\mathbf{x}}_i)_{i=1..n} \end{aligned} \tag{2}$$

Please note that neither a solution algorithm nor a quality metric for the regression is imposed by this formulation. In practice, this fitting problem is therefore often solved manually by expert assessments without following a formalized mathematical approach.

Once a suitable AEDB function has been found in terms of $f$ and $\boldsymbol{\theta}$, it can be *evaluated* to continuously *predict* the aerodynamic coefficients $\hat{\mathbf{c}}$ of the vehicle for new flight conditions $\hat{\mathbf{x}}$ that could not be observed so far. This prediction capability is requested from other technical domains and the major motivation for generating AEDBs:

$$\hat{\mathbf{c}} = f(\hat{\mathbf{x}}; \boldsymbol{\theta}) \tag{3}$$

The parametrization of the input vector $\mathbf{x}$ is however not uniquely determined, so for CALLISTO the following description has been chosen to encode the AEDB:

$$\mathbf{x} = (Ma, H, \alpha, \phi, \delta_j, \eta_j, \lambda_j, \tau, Setup)_{j=1..4} \tag{4}$$

For some aerodynamic studies of CALLISTO this parametrization has been further simplified. If, for example, the continuous transition between the vehicle configurations need not be considered, the continuous shape parameters $\eta_j$, $\lambda_j$ and $\tau$ can be replaced by a discrete categorical variable $Config$ as indicated in table 1:

$$Config \in \{\mathrm{FFO}, \mathrm{FFN}, \mathrm{UFN}, ...\} \tag{5}$$

Besides that, the categorical variable $Setup$ has been added to indicate the data generation processes behind the different aerodynamic datasets. It allows to encode possible differences in the expected error characteristics of the aerodynamic datasets during the inference phase:

$$\begin{aligned} Setup \in \{&\mathrm{TAU\ HF}, \mathrm{TAU\ LF}, \mathrm{HST}, \\ &\mathrm{TMK}, \mathrm{DATCOM}, \mathrm{FLIGHT}\} \end{aligned} \tag{6}$$

However, since most information about error characteristics are implicit expert knowledge, and furthermore this variable will be fixed to $Setup = \mathrm{FLIGHT}$ for the prediction phase, this variable might not always be listed explicitly.

In its simplest and most common realization, problem (2) is solved in a way that the prediction function (3) provides a point estimation for the nominal aerodynamic coefficients. This is often acceptable during the conceptual design phase of launch vehicles. However, when the design further matures, quantified uncertainties for these estimates will be required, especially to design a robust Guidance, Navigation & Control (GNC) system and to ensure a reliable mission architecture.

A common technique to quantify uncertainties is to extend the AEDB function (1) to interval arithmetic, so that estimated minimum and maximum values of the aerodynamic coefficients can be predicted:

$$\mathbf{c} \in [\mathbf{c}_{min}, \mathbf{c}_{max}] = f(\mathbf{x}; \boldsymbol{\theta}) \tag{7}$$

Another technique is to apply (Bayesian) probability theory to predict a probability distribution over the aerodynamic coefficients:

$$\mathbf{c} \sim p(\mathbf{c} \mid \mathbf{x}; \boldsymbol{\theta}) = f(\mathbf{x}; \boldsymbol{\theta}) \tag{8}$$

Which approach is most practical to quantify uncertainties depends on the actual use case. Interval models are well-suited for (worst) case studies and are often easier to develop due to their simple mathematical structure. Probabilistic models on the other hand are essential for Monte Carlo analyses and encode more information about parameter correlations. Here it should be noted that with a given confidence level a probabilistic model can be easily transformed into an interval model; for a reverse transformation addition assumptions about the shape of the distributions would be needed.

*Classical AEDB Generation*

Classically, the AEDB generation problem (2) is solved by expert assessments, which manually inspect the available aerodynamic datasets to determine a suitable functional relationship based on heuristics and heritage knowledge. Here, the data generation and fitting processes are often intertwined, so that test condition matrices are already selected to support easy fitting. Due to this manual approach, the classical AEDB generation process is however not standardized nor identical for every vehicle. Nevertheless, the generalized approach described in this paragraph has been observed by the authors as typical in many development projects that have reached sufficient maturity to produce flight hardware.

To simplify the fitting process, the AEDB function will be separated in a first step into a baseline functional relationship $f_{ip}$ plus multiplicative and additive correction terms:

$$f_{nom}(\mathbf{x}; \boldsymbol{\theta}) = s(\mathbf{x}; \boldsymbol{\theta}) f_{ip}(\mathbf{x}; \boldsymbol{\theta}) + b(\mathbf{x}; \boldsymbol{\theta}) \tag{9}$$

The baseline function $f_{ip}$ is then determined by low-degree interpolation, such as piecewise linear or Hermite interpolation, between a coherent subset of the available aerodynamic datapoints $\tilde{\mathbf{x}}$. This subset is commonly chosen as an equidistant grid which should cover most of the relevant flight conditions. The remaining aerodynamic datapoints will then be used to validate the generated baseline function and to determine any correction terms for scale $s$ or bias $b$, if the need for corrections seems indicated. In order to not overfit the data and to limit the workload during expert assessment, these correction terms are commonly chosen as simple constant or linear functions, which depend only on very few dimensions of the independent variables $\mathbf{x}$. For the nominal aerodynamic coefficients these terms are even frequently neglected with $s = 1$ and $b = 0$, to consider deviations between the aerodynamic datasets only during the uncertainty assessment.

In order to provide quantified uncertainties, this nominal AEDB function can be extended in a next step to determine a credible interval (7). To achieve this, minimum and maximum values for scale $s$ or bias $b$ are determined, which represent relative and absolute error bars around the nominal estimate $f_{nom}$. Please note that in this context multiplication and addition are understood in terms of interval arithmetic:

$$[\mathbf{c}_{min}, \mathbf{c}_{max}] = [s_{min}(\mathbf{x};\boldsymbol{\theta}), s_{max}(\mathbf{x};\boldsymbol{\theta})] f_{nom}(\mathbf{x};\boldsymbol{\theta}) + [b_{min}(\mathbf{x};\boldsymbol{\theta}), b_{max}(\mathbf{x};\boldsymbol{\theta})] \tag{10}$$

These relative and absolute error terms are frequently selected by graphical methods, where the nominal estimate and all relevant datapoints are plotted together. Again, simple low-dimensional constant or linear functions are commonly chosen for $s$ and $b$.

If required by the use case, the interval model for the aerodynamic uncertainties can be further extended to provide a probability distribution over the aerodynamic coefficients (8). Here, scale $s_{MC}$ and bias $b_{MC}$ are modeled as random variables which probability distributions approximate the credible intervals determined in (10):

$$\mathbf{c} = s_{MC} f_{nom}(\mathbf{x};\boldsymbol{\theta}) + b_{MC} \tag{11}$$

The simplest approach is to draw these random variables from uniform distributions $\mathcal{U}(l, r)$ over the credible interval:

$$\begin{aligned} s_{MC} &\sim \mathcal{U}(s_{min}(\mathbf{x};\boldsymbol{\theta}), s_{max}(\mathbf{x};\boldsymbol{\theta})) \\ b_{MC} &\sim \mathcal{U}(b_{min}(\mathbf{x};\boldsymbol{\theta}), b_{max}(\mathbf{x};\boldsymbol{\theta})) \end{aligned} \tag{12}$$

However, this model creates a distribution with sharp boundaries without any probability mass outside the interval, which is often undesirable in practice. Such a model also neglects any concentration of probability mass close to the nominal value. Therefore, is also common to approximate the credible interval with the $z_\alpha\sigma$-interval of a Gaussian distribution $\mathcal{N}(\mu, \sigma)$ for a given confidence level $\alpha$:

$$\begin{aligned} s_{MC} &\sim \mathcal{N}\left(\frac{s_{max}(\mathbf{x};\boldsymbol{\theta}) + s_{min}(\mathbf{x};\boldsymbol{\theta})}{2}, \frac{s_{max}(\mathbf{x};\boldsymbol{\theta}) - s_{min}(\mathbf{x};\boldsymbol{\theta})}{2z_\alpha}\right) \\ b_{MC} &\sim \mathcal{N}\left(\frac{b_{max}(\mathbf{x};\boldsymbol{\theta}) + b_{min}(\mathbf{x};\boldsymbol{\theta})}{2}, \frac{b_{max}(\mathbf{x};\boldsymbol{\theta}) - b_{min}(\mathbf{x};\boldsymbol{\theta})}{2z_\alpha}\right) \end{aligned} \tag{13}$$

The classical approach has the main advantage to generate AEDB functions with a simple mathematical structure. This way, good understanding of the implemented error terms can be ensured to avoid overfitting or hidden issues. Also, heritage and expert knowledge can be easily incorporated without complicated mathematical formalization. The resulting prediction function for the aerodynamic coefficient usually has a high computational performance, so that it can be evaluated online during simulations of other technical domains or even during flight on the onboard computer.

On the other hand, the fitting process for this classical approach is difficult to automate, particularly the selection of error terms $s$ and $b$ as noted in (10). Therefore, a lot of expert's workforce needs to be invested, which make frequent refitting to new data not practical. Also, the actual selection of error term is not traceable and may subjectively vary between experts. Due to the simple mathematical structure and the manual fitting process, complex error contributors, which depend on multiple dimensions, are relatively difficult to identify and to consider. Particularly regarding the probabilistic uncertainties model (11) - (13), statistical correlation between errors are completely neglected by this simple extension of the interval model.

*Introduction to Bayesian Inference*

The other approach for AEDB generation, which will be presented in this paper, applies Bayesian Inference to solve the AEDB generation problem (2). In the following paragraphs a short introduction will be given to this methodology.

*Bayesian Inference* is a general method to update the probability distribution of a statistical model based on observations by the application of Bayes' law. In contrast to classical frequentest statistics, where models and parameter are assumed to be fixed and fitted to a number of repeated experiments, uncertainties in Bayesian statistics are explicitly quantified by probability distributions over all levels of the model, which can be updated with any amount of observable data. Due to this very general approach, also non-repeatable phenomena can be modeled statistically with Bayesian inference. In the last decades, this approach has found a wide range of applications through various fields of science, engineering, medicine, philosophy, sport and others.

The general Bayesian workflow can be summarized in the following steps:

1. To specify a statistical model for the phenomena under investigation and to determine the *likelihood function* of this model, which relates the model specific parameters to the observable data;
2. To encode a-priori expert knowledge on the model parameters through a *prior probability distribution* which represents the available information before data collection;
3. To combining the prior distribution and the likelihood function for an observed set of data via Bayes' Theorem, to determine the *posterior distribution* which represents the now updated knowledge about the model parameters.
4. To predict the expected distribution of new, unobserved data via calculating the *posterior predictive distribution* from the posterior distribution

For the inference step, which derives the posterior distribution as a consequence of the prior probability and the likelihood function, Bayes' theorem can be formulated as:

$$p(\boldsymbol{\theta} \mid \tilde{\mathbf{z}}_{i=1..n}, \boldsymbol{\alpha}) = \frac{p(\tilde{\mathbf{z}}_{i=1..n} \mid \boldsymbol{\theta}, \boldsymbol{\alpha}) p(\boldsymbol{\theta} \mid \boldsymbol{\alpha})}{\int p(\tilde{\mathbf{z}}_{i=1..n}, \mid \boldsymbol{\theta}, \boldsymbol{\alpha}) p(\boldsymbol{\theta} \mid \boldsymbol{\alpha})\, d\boldsymbol{\theta}} \tag{14}$$

where

- $\tilde{\mathbf{z}}_{i=1..n}$ is the set of observed data samples;
- $\boldsymbol{\theta}$ is the vector of *parameters* for the data point's distribution, i.e. $z \sim p(z|\boldsymbol{\theta})$;
- $\boldsymbol{\alpha}$ is the vector of any *hyperparameters* for the parameter's distribution, i.e. $\boldsymbol{\theta} \sim p(\boldsymbol{\theta}|\boldsymbol{\alpha})$;
- $p(\boldsymbol{\theta} \mid \boldsymbol{\alpha})$ is the *prior distribution* which is the expected probability of the model parameters before inference
- $p(\tilde{\mathbf{z}}_{i=1..n} \mid \boldsymbol{\theta}, \boldsymbol{\alpha})$ is the *likelihood function*, which determines the relationship between observed datapoints and model parameters

- $p(\boldsymbol{\theta} \mid \tilde{\mathbf{z}}_{i=1..n}, \boldsymbol{\alpha})$ is the *posterior distribution* which is the probability of the model parameters that has been inferred from the data.

In most use cases the inferred posterior distribution over the model parameters is not the primary quantity of interest, but rather the expected distribution for new datapoints. This information can be retrieved from posterior predictive distribution, which depends on the posterior distribution:

$$p(\hat{\mathbf{z}} \mid \tilde{\mathbf{z}}_{i=1..n}, \boldsymbol{\alpha}) = \int p(\hat{\mathbf{z}} \mid \boldsymbol{\theta}, \boldsymbol{\alpha}) p(\boldsymbol{\theta} \mid \tilde{\mathbf{z}}_{i=1..n}, \boldsymbol{\alpha}) \, d\boldsymbol{\theta} \quad (15)$$

For most real-world problems, equations (14) and (15) cannot be solved analytically, but need to be approximated by numerical algorithms. PyMC [25], [26] is a probabilistic programming package for Python that allows users to fit Bayesian models using a variety of numerical methods, most notably Markov Chain Monte Carlo (MCMC) and Variational Inference (VI) algorithms. Along with core sampling functionality, PyMC includes methods for summarizing output, plotting, goodness-of-fit and convergence diagnostics. Its development began in 2003, as an effort to generalize the process of building Metropolis-Hastings samplers, with an aim to making MCMC more accessible to non-statisticians. PyMC includes a large suite of well-documented statistical distributions and also includes a module for modeling Gaussian processes. In the scope of this study, PyMC will therefore be used to implement Bayesian models and to conduct inference and predictions tasks.

*Introduction to Gaussian Processes*

A common class of models that are used in Bayesian contexts are Gaussian Process (GP) models. Here, a Gaussian process is applied to model a functional behavior within the provided dataset. Gaussian processes are formally an extension of the Multivariate Normal Distribution (MVN) to infinite dimensions, therefore defining a probability distribution over a function space. With a *mean function* $m(x)$ and a *covariance function* or *kernel* $k(x, x')$, such a model is commonly denoted as:

$$f(x) \sim \mathcal{GP}\left(m\left(x\right), k\left(x, x'\right)\right) \quad (16)$$

The selection of $m(x)$ and $k(x, x')$ restricts the shape of functions $f(x)$ that can be drawn for this distribution. Therefore, GP models are often used for Bayesian Inference, since plenty different functional relationships can be modeled just by adequate selection of $m(x)$ and $k(x, x')$. Heuristically it has be observed, that most of the information about a Gaussian process is encoded in the covariance function, so that without loss of generally $m(x) = 0$ can often be assumed.

Many well-known kernels are described in literature, which can be further combined to more complex covariance function [27], [28]. This way, it is common for Bayesian models to encode a-priori knowledge via combined and tailored covariance functions. A short overview of the kernels that are used in the scope of this paper, is given in the following paragraphs.

Squared-Exponential (SE) kernel, also known as the *Radial Basis Function* kernel, is one of the most popular kernels for GP. It has the form:

$$k_{\mathrm{SE}}\left(x, x'\right) = \exp\left(-\frac{\left(x - x'\right)^2}{2l^2}\right) \quad (17)$$

Here $l$ is the length scale which determines the length of the 'wiggles' in the function. No significant correlation is given between function values that are more than $l$ units away from each other.

The class of *Matern* kernels is a generalization of the aforementioned SE kernel. It has an additional parameter $\nu$ which controls the smoothness of the resulting function: The smaller $\nu$, the less smooth the approximated function. It can be shown that the sampled functions are $t$-times mean-square differentiable if and only if $\nu > t$. As $\nu \to \infty$, the kernel becomes equivalent to the SE kernel. [27] For the approximation of physical processes, Matern-3/2 (M32) with $\nu = 3/2$ and Matern-5/2 (M52) with $\nu = 5/2$ are popular kernel choices. The M52 kernel is for example defined as:

$$\begin{aligned} k_{\mathrm{M52}}\left(x, x'\right) = &\left(1 + \frac{\sqrt{5}}{l}\|x - x'\| + \frac{5}{3l^2}\|x - x'\|^2\right) \\ &\exp\left(-\frac{\sqrt{5}}{l}\|x - x'\|\right) \end{aligned} \quad (18)$$

The White Noise (WN) kernel represents independent and identically distributed noise added to the Gaussian process distribution:

$$k_{\mathrm{WN}}(x, x') = \nu^2 \delta(x, x') \quad (19)$$

where $\nu^2$ is the variance of the noise and $\delta(x, x')$ is the Kronecker delta, returning 1 if $x = x'$ else 0. This results in a covariance matrix with zeros everywhere except on its diagonal, which contains the variances.

*Coregionalization* is an idea used in situations where not all function outputs could be observed for a particular input. However, the resulting Coregion (CR) kernel is also well suited to construct kernels over discrete categorical variables. For a matrix $\mathbf{B}$ defined as

$$\mathbf{B} = \mathbf{W}\mathbf{W}^{\intercal} + \mathrm{diag}\left(\kappa\right) \quad (20)$$

the CR kernel returns the element of the matrix which index is given by the input variables:

$$k_{\mathrm{CR}}(x, x') = \mathbf{B}[x, x'] \quad (21)$$

*Warped Input* kernel can be used to transform the inputs of any kernel to another domain by applying an arbitrary function $w(x)$.

$$\tilde{k}(x, x') = k(w(x), w(x')) \quad (22)$$

This approach is commonly used to transform input data from a periodical domain to kernels that are operating on an euclidean domain. [29]

Combining Kernels is a common way to fit the data accordingly if more than one type of feature is present. *Multiplying Kernels* is the standard way to combine two different kernels especially if they are defined on different inputs dimensions of the function. This operation reflects a standard AND operation. So if two kernels are multiplied, then the resulting kernel will have a high value if and only if both the base kernels have a high value. *Adding Kernels* analogously can be thought of as an OR operation. That is, if two kernels are added, then the resulting kernel will have a high value if either of the two base kernels has a high value.

*Bayesian AEDB Generation*

In contrast to the classical approach for AEDB generation, the Bayesian approach is an inherently probabilistic method which incorporates the description of uncertainties right from the beginning. As such, the AEDB function is modeled as a probability distribution over the aerodynamic coefficients vector $\mathbf{c}$, dependent on the generalized input vector $\mathbf{x}$, the generalized parameter vector $\boldsymbol{\theta}$ and hyperparameter vector $\boldsymbol{\alpha}$, as well as on the datapoints that have been used for fitting $(\tilde{\mathbf{c}}_i, \tilde{\mathbf{x}}_i)_{i=1..n}$:

$$\mathbf{c} \sim p(\mathbf{c} \mid \mathbf{x}; (\tilde{\mathbf{c}}_i, \tilde{\mathbf{x}}_i)_{i=1..n}, \boldsymbol{\theta}, \boldsymbol{\alpha}) \tag{23}$$

To generate such a Bayesian AEDB, at first a prior predictive model is developed to determine the actual parametrization of $\boldsymbol{\theta}$, which shall be fitted during Bayesian Inference:

$$p(\mathbf{c}, \mathbf{x} \mid \boldsymbol{\alpha}) = \int p(\mathbf{c}, \mathbf{x} \mid \boldsymbol{\theta}) p(\boldsymbol{\theta} \mid \boldsymbol{\alpha})\, d\boldsymbol{\theta} \tag{24}$$

At this stage expert knowledge can be encoded in the model, either by selecting the structure of the likelihood $p((\mathbf{c}, \mathbf{x})|\boldsymbol{\theta})$ and the prior distribution $p(\boldsymbol{\theta}|\boldsymbol{\alpha})$, or by the provision of values for the hyperparameters $\boldsymbol{\alpha}$. Especially GP models have been proven here as an effective class of likelihood functions, since they can be adapted to model very different functional behaviors but still provide good interpretability for experts. The encoded a-priori knowledge can remain very broad, just encoding some general properties of the AEDB function.

It should be noted that in Bayesian models also the parameter vector $\boldsymbol{\theta}$ is treated as a random variable. According to equation (14) the posterior distribution over these parameters can be inferred from the likelihood over the provided training data and from the prior distribution:

$$p(\boldsymbol{\theta} \mid (\tilde{\mathbf{c}}_i, \tilde{\mathbf{x}}_i)_i, \boldsymbol{\alpha}) = \frac{p((\tilde{\mathbf{c}}_i, \tilde{\mathbf{x}}_i)_i \mid \boldsymbol{\theta}, \boldsymbol{\alpha}) p(\boldsymbol{\theta} \mid \boldsymbol{\alpha})}{\int p((\tilde{\mathbf{c}}_i, \tilde{\mathbf{x}}_i)_i \mid \boldsymbol{\theta}, \boldsymbol{\alpha}) p(\boldsymbol{\theta} \mid \boldsymbol{\alpha})\, d\boldsymbol{\theta}} \tag{25}$$

Since for most Bayesian models this equation cannot be solved analytically in a closed form, several approximation methods have been developed and implemented in software libraries, such as PyMC. The inference process for the Bayesian AEDB can therefore be fully automated, requiring computational resources only.

Once the posterior distribution $p(\boldsymbol{\theta}|(\tilde{\mathbf{c}}_i, \tilde{\mathbf{x}}_i)_i, \boldsymbol{\alpha})$ has been inferred (or sufficiently approximated), it can be used to calculate the posterior predictive distribution, which determines a probability distribution over the aerodynamic coefficients $\mathbf{c}$ for any flight condition $\mathbf{x}$.

$$p(\hat{\mathbf{c}}, \hat{\mathbf{x}} \mid (\tilde{\mathbf{c}}_i, \tilde{\mathbf{x}}_i)_i, \boldsymbol{\alpha}) = \int p(\hat{\mathbf{c}}, \hat{\mathbf{x}} \mid \boldsymbol{\theta}) p(\boldsymbol{\theta} \mid (\tilde{\mathbf{c}}_i, \tilde{\mathbf{x}}_i)_i, \boldsymbol{\alpha})\, d\boldsymbol{\theta} \tag{26}$$

For subsequent statistical analyses, e.g. Monte Carlo simulations of the flight trajectory, the posterior predictive distribution or samples thereof can directly be used as input. If however an interval model as in (7) is requested, the Highest Density Interval (HDI) or Equal-Tailed Interval (ETI) can be calculated from the distribution for a given confidence level. Furthermore, a point-estimate of the nominal AEDB value can be determined by the mean or median of the distribution.

The main advantage of this Bayesian approach is that the model inference and prediction steps can be fully automated, so that the required workforce from experts might be reduced significantly. This way frequent refitting of the AEDB function would be possible whenever new data arrives. Also, more complex relationships and correlations of the uncertainty contributors can be inferred directly from the available data, depending on very broad a-priori knowledge only.

On the other hand, the translation of available expert knowledge is more complicated than for the Classical AEDB, since it needs to be mathematically formalized and encoded in the prior distributions. Therefore and due to the quite complex structure of the model, the results might also be more difficult to interpret which increases the risk for hidden issues in the model structure or in the fitting process. Even though less human workforce is required for fitting the Bayesian model, significant computational performance is required for inference and prediction, which makes it likely difficult to be executed online during simulation or flight.

*Related Work*

Generating an aerodynamic database is an intrinsic part of every launch vehicle development program and for the design of a robust GNC system, the uncertainties of the AEDB have to be assessed. With regard to RLVs, the extensive work done for the AEDB generation, including estimation of the uncertainties, for the Space Shuttle program is the most completely published example [30]. The aerodynamic coefficients in this case were derived based solely on WTT, with extensive campaigns in multiple facilities in order to cover the entire flight envelope of the vehicle. The scatter within the data of multiple WTT facilities was defined as the so-called tolerance, the lower uncertainty bound. Additional uncertainties, to account for systemic errors in wind tunnel tests compared to full scale vehicles, were defined as an upper uncertainty bound, called variations. These were sized based on the comparison of pre-flight WTT data with post-flight data from previous similar configurations. A challenge with this approach is the limited number of applicable and available datasets, especially in the hypersonic regime [31].

In modern vehicle developments the massive effort of this extensive WTT approach is usually not undertaken. Instead, CFD data is often combined with data from WTTs in order to reduce costs and accelerate the development program. However, the number of modern development programs that

have published their methodology is limited. Current winged flight experiments, like ReFEx [32] or HEXAFLY-INT [33], rely heavily on CFD data of various fidelity for the generation of their AEDB. Here, WTT data is mostly used to crosscheck the CFD data and to estimate the uncertainty associated with the resulting database. The AEDB of the expandable launcher VEGA-C [34] has been developed with a similar approach, but used the generated WTT polars as the underlying dataset for sub- and supersonic velocities. Correction terms and uncertainty levels were subsequently estimated by comparison with various CFD results.

Stradtner et al. [35] presented a surrogate modelling framework to obtain aerodynamic stability and control data sets at an early design phase based on the data fusion of low and high fidelity CFD data. In contrast to the work presented herein with datasets generated a-priori, an adaptive sampling process is employed to reach a required uncertainty level. This approach could be used in a future extension of the current work in order to select additional points of interest for further CFD simulations or WTT experiments. The automated process presented within [35] is limited to CFD data, since WTT datasets cannot easily be generated in the loop.

Renganathan et al. [36] have applied Bayesian methods for data fusion of WTT and CFD data in the context of aerodynamics. In contrast to this work, the focus was on the local pressure distribution along an airfoil, not on the aerodynamic coefficients of an entire vehicle. The two datasets were fused with Bayesian Inference in order to estimate the true field that best matches the measured quantities. The work shares the same fundamental challenge with the study shown herein that this true field is unknown and can only be estimated.

Specific to vehicles using retro-propulsion, while commercial vehicles similar to CALLISTO are currently operational, their workflow and methods are not published.

Work on aerodynamic datasets is, of course, not limited to the descent of the vehicles, the ascent of launch vehicles is also analyzed, albeit with different goals. The focus is usually less on controllability, due to the large control authority achieved through the active rocket engines, and more on the characterization on mechanical and thermal loads [37].

While not commonly used for the assessment of uncertainties of launch vehicles AEDBs, Bayesian Inference and Gaussian Process Models have been successfully applied to several interdisciplinary tasks for science, engineering, philosophy, medicine, sport, and law applications. The following list highlights some selected use cases that share similarities with the approach described above.

Gaussian Processes have been shown to be very useful in the problem avoidance of scrap and adherence to tolerances in forging super-alloys. Hoffer et al. [38] have shown that they can be used to replace the established Finite Element Method (FEM) models which require extensive computational resources. The Gaussian process model acted as a robust substitute which resulted in a fast estimation that adequately depicts reality and was shown to be over 3000 times faster compared to FEM simulations, with an acceptable loss of accuracy and information.

Morita et al. [39] have shown that Bayesian optimization with Gaussian process regression can be successfully used for CFD aeroshape optimization problems. It should be noted that the Bayesian optimization is among the gradient-free approaches and hence only requires forward evaluation of the quantities of interest, i.e. running of resource-intensive CFD code.

Deep Bayesian Gaussian Processes have also been used for uncertainty estimation in electronic health records. Through a series of experiments on prediction of the first incidence of heart failure, diabetes and depression applied to large-scale electronic medical records, Li et al. [40] demonstrate that their method is better at capturing uncertainty than deep Bayesian neural networks in terms of indicating data insufficiency and identifying misclassifications, with a comparable generalization performance.

Bayesian Inference and Gaussian Processes are also used for quite novel methods in sports like the work by Zhao et al. [41] which analyzed kernel based machine learning methods, specifically Gaussian Process, to analyze the forces in cross country skiing races.

In general, the Bayesian approach developed in this paper is novel for the generation of AEDBs regarding the prediction of coefficient for entire vehicles including the quantification of uncertainties. In other fields with similar problem types, the applied methodologies have shown considerable effectiveness.

## 4. MODEL DEFINITION

During the detailed design phase of CALLISTO several Bayesian models have been tested on different aspects of the AEDB. In this paper, we will focus on the comparison of one typical *Bayesian Model* with the classical *Reference Model* to assess the feasibility of the Bayesian approach. The selected Bayesian model incorporates many common characteristics that have also been observed in other tested models.

In order to focus on the actual comparison of methodologies, we have furthermore restricted the problem space to model the normal force coefficient $C_z$ in dependency of the Angle of Attack $\alpha$ for the UFN configuration only. For the following chapters the considered models and datasets will therefore be limited to the below-mentioned ranges or values:

$$\begin{aligned} Ma &= 0.5 \\ H &= 1000\mathrm{m} \\ \alpha &\in [0^\circ..360^\circ] \\ \phi &= 0^\circ \\ \delta_{j=1..4} &= 0^\circ \\ Config &= \mathrm{UFN} \end{aligned} \tag{27}$$

The rationale for this restriction is to maintain a relatively simple model structure and to present well-interpretable first results. More complex models have been tested, but due to the curse of dimensionality the computational requirements for inference and prediction, as well as the challenge of visualizing the results significantly increase with the number of input and output dimensions. For the initial comparison of methodologies this complexity is however not required. A full Bayesian characterization of CALLISTO's AEDB is planned for future publication.

The choice of the flight conditions in (27) has been driven by two aspects. First, these conditions correspond to a typical point on the descent trajectory of CALLISTO during the aerodynamically controlled flight phase. Uncertainties in this domain can be considered most critical for CALLISTO's design, since a pinpoint landing on the landing pad needs to be reached even under off-nominal conditions. Therefore, the GNC design relies on a robust quantification of uncertainties in this domain. Second, a relatively large number of aerodynamic datapoints are available for these conditions, from all CFD and WTT sources as shown in section 2. This supports the validation of the inference results, allowing conclusions with regard to the model quality to be drawn.

*Bayesian Model*

The Bayesian model that is analyzed in this paper is defined as a GP over normal force coefficient $C_z$ in dependency of the Angle of Attack $\alpha$ and the categorical variable $Setup$. The later dependency is used to model the fact that aerodynamic datasets from different sources do not share identical error characteristics. For mathematical convenience, this categorical variable has been encoded as a discrete integer $m$ which enumerates each element of the domain (6) with a unique value:

$$C_z(\alpha, m) \sim \mathcal{GP}(\mathrm{o}, k) \tag{28}$$

Whereas a zero mean function is assumed for the GP, the covariance function is constructed by the combination of several elementary kernels:

$$\begin{aligned} k(\alpha, m, \alpha', m') &= \eta^2 k_{\mathrm{SE}}(w(\alpha), w(\alpha'); l_s) \\ &\quad + k_{\mathrm{CR}}(m, m'; \mathbf{B}) k_{\mathrm{M52}}(w(\alpha), w(\alpha'); l_n) \\ &\quad + k_{\mathrm{WN}}((\alpha, m), (\alpha', m'); \nu) \\ \mathbf{B} &= \mathrm{diag}(\sigma^2_{m=1..6}) \\ w(\alpha) &= (\sin\alpha, \cos\alpha)^\intercal \end{aligned} \tag{29}$$

Here, the SE kernel models the underlying global behavior of the AEDB function. The M52 kernel on the other hand models any deviation of the aerodynamic data points from this global behavior. Due to the multiplication with the CR kernel, this error behavior is treated separately for each $Setup$. Furthermore, both continuous kernels have been warped to the periodic AoA domain via $w(\alpha)$. The selection of these two kernels was driven by the assessment that both induce relatively smooth functions [27], since a discontinuous or non-differentiable behavior of the AEDB is not expected. The final WN kernel models any remaining variability, for example due to measurement noise or truncation errors, and helps to stabilize the numerical convergence of the inference algorithm. Its inferred variance is however very low, so this term could be neglected for most practical considerations.

Regarding the prior distributions, it is assumed that all parameters in (29) are drawn from an Inverse Gamma distribution $\mathcal{IG}$:

$$\eta, \sigma_{m=1..6}, \nu, l_s, l_n \sim \mathcal{IG}(a, b) \tag{30}$$

This selection has been made by heuristic considerations to have a positive domain for each parameter with very small probability mass close to zero. [42] The shape $a$ and scale $b$ parameters have been selected individually by expert assessment, so that weakly informative priors are constructed with mean values in the expected order of magnitude for each parameter. [43]

The full Bayesian Model (28) - (30) has been implemented with PyMC in Python. This implementation supports parameter inference and posterior prediction via an MCMC algorithm. With this approach, all prior, posterior and posterior predictive distributions are approximated via sampling. For diagnostic purposes, metrics about the approximation and convergence quality are also directly provided by this implementation.

*Reference Model*

As reference for the Bayesian Model, the classically generated AEDB model will be used which is so far the global baseline for the development process of CALLISTO. A detailed description about the development and the structure of this model is given in [13].

This Reference Model is constructed from a piecewise linear interpolation of the TAU LF dataset. Few correction terms to this interpolation, as denoted in (9), have been identified and complemented, e.g. to model the impact of engine throttling or Thrust Vector Control (TVC). In this context, also the applied superposition principle to model the fin deflections can be interpreted as correction terms. However, due to the restriction of the problem space (27) none of these corrections will be active in the scope of this paper, so that the interpolated function $f_{lip}$ can directly be seen as the estimator for the nominal value. This way, the Reference Model can be formulated as:

$$C_z(\alpha) = f_{lip}(\alpha; (\tilde{C}_{z,i}, \tilde{\alpha}_i)_{TAULF}) + b_{MC}(\alpha) \tag{31}$$

In order to quantify the uncertainty in this model, constant absolute error $e_{abs}$ and relative error $e_{rel}$ terms have been defined by expert assessments. However, both terms have formally been applied as a bias $b$, since only the maximum effective error in dependency of the AoA shall be considered:

$$b(\alpha) = \pm \max\{|e_{rel} f_{lip}(\alpha_i; (\tilde{C}_{z,i}, \tilde{\alpha}_i)_{TAULF})|, |e_{abs}|\} \tag{32}$$

Applying the probabilistic approximation of this interval (13) under consideration of $3\sigma$-confidence for its estimation, the probabilistic bias $b_{MC}$ can be defiend as:

$$b_{MC}(\alpha) \sim \mathcal{N}(\mathrm{o}, \frac{1}{3}|b(\alpha)|) \tag{33}$$

The full classical Reference Model has been implemented and validated in Matlab, primarily to be use for Monte Carlo campaigns of different subsystems. This implementation supports predictive sampling, but also nominal and interval estimates can be generated for any flight conditions. It should be noted that this implementation supports all flight conditions of CALLISTO, not only from the restricted problem space (27). Since this model has been classically generated, automated parameter inference is obviously not supported.

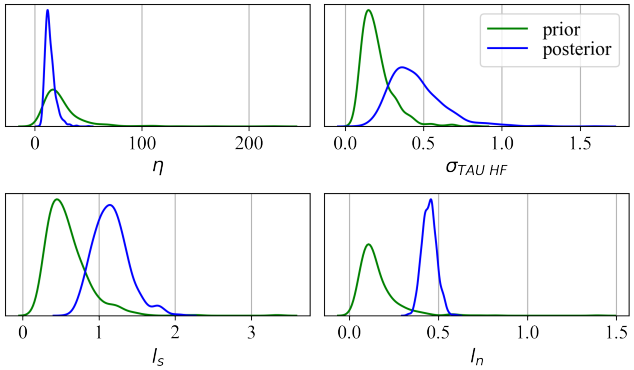


**Figure 5**. Comparison of prior and posterior distributions over some selected parameters of the Bayesian Model.

## 5. Inference Results

To allow a first comparison of the Bayesian approach with the classical approach for generating AEDBs, the software implementation of the *Bayesian Model* and *Reference Model* described in section 4 have been evaluated and further analyzed. These results are presented in the following paragraphs and compared.

Since Bayesian Inference is a new approach in this field, the intention is on one hand to demonstrate the behavior of the Bayesian Model during inference, so that the validity of the model and its results can be concluded. For the Reference Model such a demonstration cannot be done, since this model is inherently provided in a (manually) fitted state. On the other hand, it shall be assessed whether the predictive capabilities for unknown flight conditions are equally good for both models, or if advantages or issues can be observed for one or the other model. Finally, a very short comparison of the resources necessary for inference and prediction with both models is given.

*Comparison of Prior and Posterior Distributions*

By application of Bayes Law (25) during the inference phase, the probability distribution over the model parameters will be moved from the prior distribution (30) to the posterior distribution.

For the PyMC implementation of the Bayesian Model, this posterior distribution is approximated with a MCMC algorithm. This way equation (25) does not need to be solved analytically, but rather a set of samples is generated which converges towards the searched posterior distribution. For the scope of this study, all probability distributions are approximated by 4000 samples which have been drawn by 4 independent chains. The usage of few independent chains is quite common for this class of algorithms to avoid, or at least to discover, any possible convergence issues of the algorithm.

Figure 5 illustrates the approximated Probability Density Function (PDF) of the posterior distributions for some selected model parameters, compared to their prior distributions. It can be seen that due to inference on the provided aerodynamic datasets, the distributions over the parameter space have evolved in location, scale and shape. However, a significant overlap in the probability mass distribution can still be observed for each posterior and prior, with a slight exception for length scale $l_n$. This overlap can be interpreted as an indicator that the prior distributions were chosen well. Whereas for some parameters like $\eta$ the uncertainty has been narrowed down by the dataset, the uncertainty of other parameters like $\sigma_{\text{TAU HF}}$ has increased during inference. Furthermore, it should be noticed that for some prior distributions a small probability mass fraction is plotted over slightly negative values. This is however just an artifact of the shown visualization, as the drawn MCMC samples are smoothed by Kernel Density Estimation (KDE) for illustration purposes. The definition of the prior (30), as well as all prior and posterior samples are in the positive domain.

**Table 2**. Summary statistics of the prior and posterior distributions over all model parameters of the Bayesian Model.

| Parameter | | Mean | SD | 95% HDI | |
|---|---|---|---|---|---|
| $\eta$ | prior | 25.533 | 22.037 | 6.404 | 64.674 |
| | posterior | 14.327 | 4.924 | 6.943 | 23.655 |
| $\sigma_{\text{TMK}}$ | prior | 0.205 | 0.094 | 0.064 | 0.385 |
| | posterior | 1.311 | 0.492 | 0.563 | 2.311 |
| $\sigma_{\text{HST}}$ | prior | 0.199 | 0.109 | 0.068 | 0.375 |
| | posterior | 2.013 | 0.581 | 1.016 | 3.158 |
| $\sigma_{\text{TAU HF}}$ | prior | 0.203 | 0.102 | 0.067 | 0.402 |
| | posterior | 0.444 | 0.161 | 0.172 | 0.756 |
| $\sigma_{\text{TAU LF}}$ | prior | 2.027 | 0.954 | 0.790 | 4.166 |
| | posterior | 2.804 | 0.629 | 1.673 | 4.032 |
| $\sigma_{\text{DATCOM}}$ | prior | 19.408 | 10.032 | 6.989 | 38.449 |
| | posterior | 2.038 | 0.287 | 1.519 | 2.593 |
| $l_s$ | prior | 0.592 | 0.295 | 0.212 | 1.158 |
| | posterior | 1.162 | 0.240 | 0.712 | 1.630 |
| $l_n$ | prior | 0.156 | 0.115 | 0.036 | 0.349 |
| | posterior | 0.447 | 0.040 | 0.370 | 0.524 |
| $\nu$ | prior | 0.102 | 0.081 | 0.024 | 0.235 |
| | posterior | 0.005 | 0.000 | 0.004 | 0.006 |

A summary statistic of the prior and posterior distributions for all model parameters is given in table 2.

*Comparison of Posterior Predictive Distributions*

The main application of any AEDB function, and the major motivation for their development, is the prediction of aerodynamic coefficients for flight conditions not specifically covered by the existing dataset. In a Bayesian setup this is done by the posterior predictive distribution (26), but also classical probabilistic models (11) can be used similarly.

For the Bayesian Model, the posterior predictive distribution is visualized in figure 6 for the full AoA domain. Here, the PDF is shown by the reddish colormap, while a selection of sample realizations are plotted in light gray. It can be seen that the distribution has adapted the typical periodic behavior during inference, which is expected for the normal force coefficient $C_z$ in dependency on $\alpha$. Globally, all datapoints have been fitted quite well, just for the DATCOM data a bias can be observed. Whereas the spread of the distribution is relatively large for most AoA, it significantly narrows down in the region $\alpha \approx 160°...200$ where HST, TMK and TAU HF data are available for inference. Furthermore, the plotted sample realizations show some noise and variability with respect to the AoA, but most realizations remain close to the mean function.

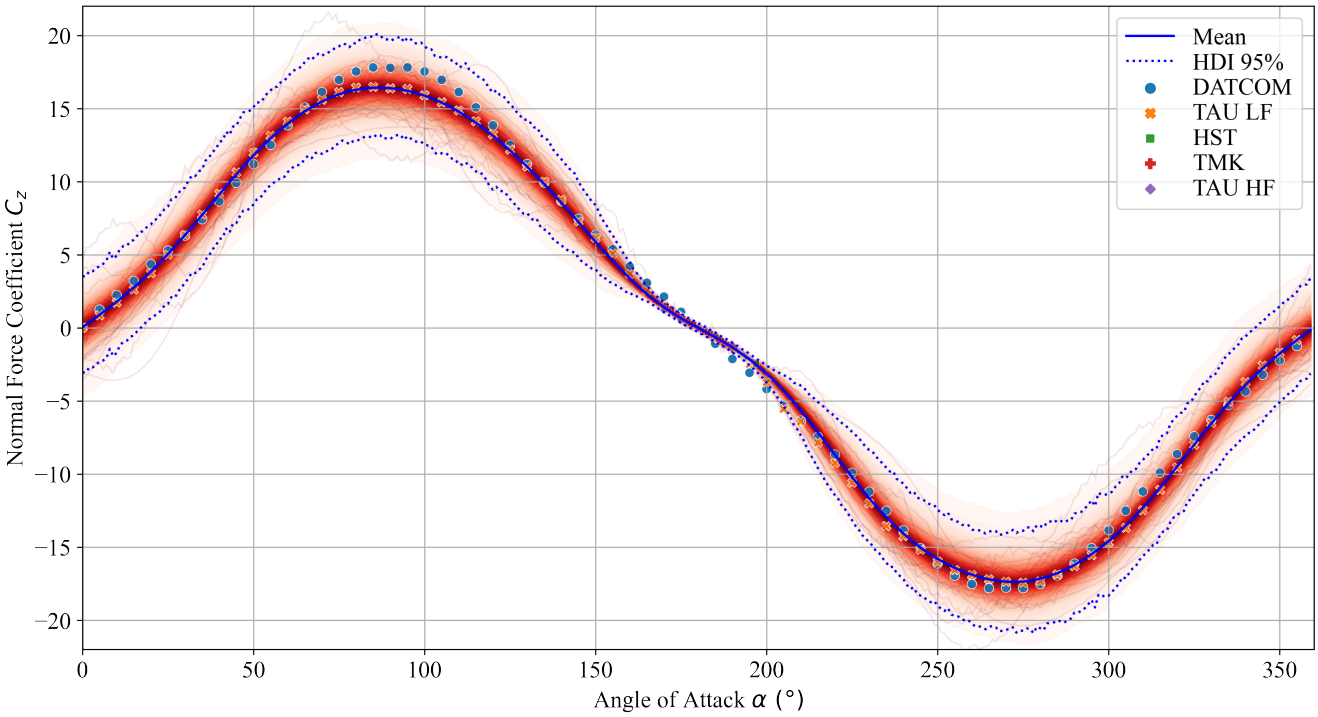


**Figure 6**. Posterior predictive distribution of the Bayesian Model in comparison with the aerodynamic datasets.

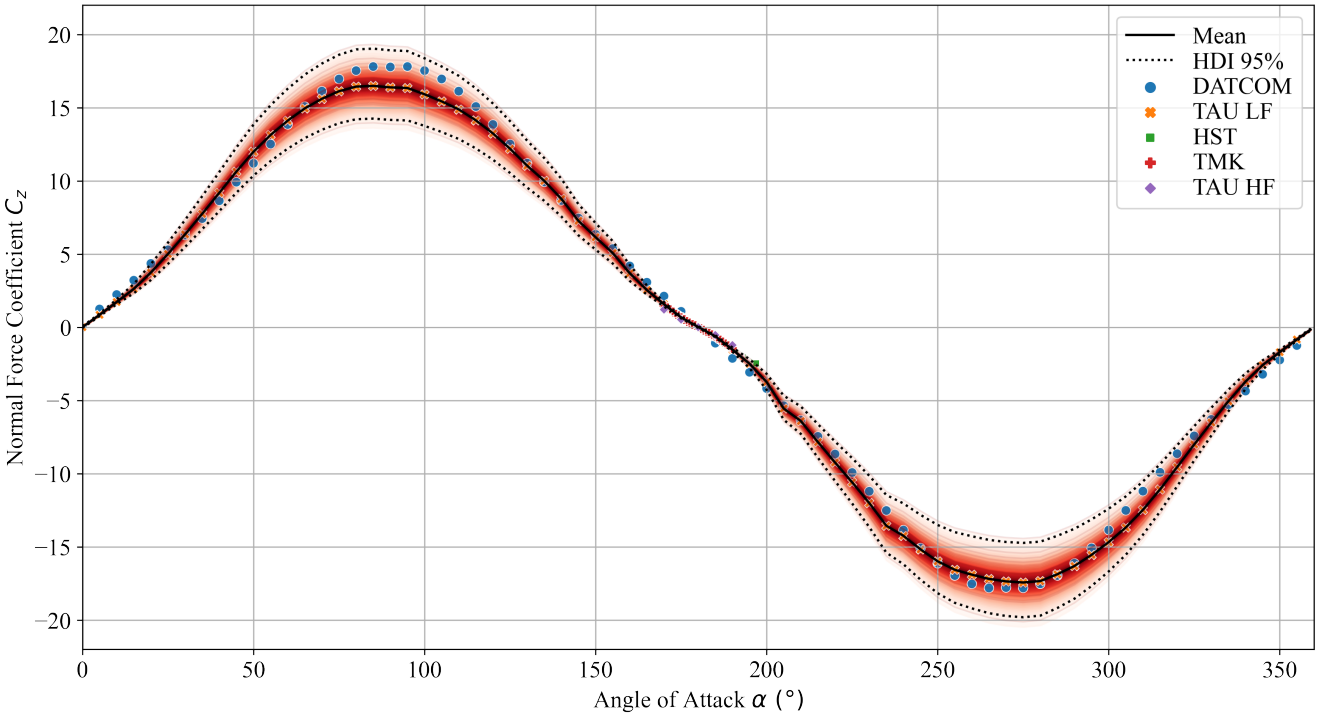


**Figure 7**. Posterior predictive distribution of the classical Reference Model in comparison with the aerodynamic datasets.

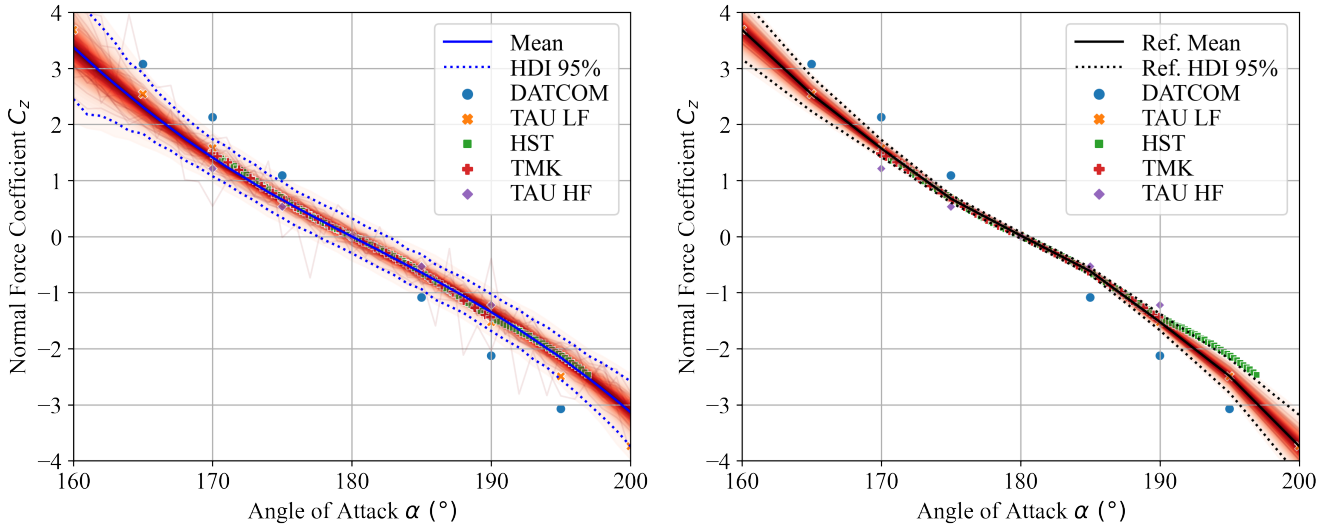


**Figure 8**. Comparison of the posterior predictive distributions for $\alpha = 160°...200$. Left: Bayesian Model; Right: Classical Reference Model.

For direct comparison, a similar plot of the posterior predictive distribution of the Reference Model is given in figure 7. Also here, the typical periodic behavior is reflected by the probability distribution. Whereas the TAU LF datapoints are fitted perfectly by the mean function, as expected by the construction of the Reference Model, again a bias towards the DATCOM dataset can be observed. As for the Bayesian model, the spread of the distribution is relatively large around $\alpha \approx 90°$ and $\alpha \approx 270°$, while it narrows down around $\alpha \approx 180°$ In contrast however, the spread of the Reference model also narrows down around $\alpha \approx 0°$ This can be a sign that additional high fidelity data is available here for fitting, that has just not been provided to the Bayesian Model, or that this is just an artifact from the simple structure of the Reference Model. It can however be observed that the spread of Reference Model is generally smaller than the spread of the Bayesian Model, for all AoA. Looking at the plotted sample realizations, it can be seen that they are all parallel to the mean function, showing no variability with respect to the AoA besides the global behavior. This indicates a very strong correlation between predictions from neighboring AoAs. Whether such a variability is a desired feature of the AEDB or not, is a point that should be further elaborated with the AEDB users.

A more detailed investigation of the posterior predictive distributions in the region $\alpha \approx 160°...200$ is given in figure 8. Again, it can be observed that the spread of the Bayesian Model is significantly larger than for the Reference Model. However, all datapoints (with exception of DATCOM) are well-covered by the 95% HDI interval of the Bayesian Model, whereas for the Reference Model several HST and TAU HF datapoints are outside this interval. This different behavior of both models can be seen as a typical instantiation of the well-known bias-variance dilemma. [44] According to this principle, it is not possible for any regression problem to minimize the variance and the bias at the same time. If the variance is decreased by different parameter selections, the bias will automatically increase at the same time. Since this trade-off is difficult to solve, a clear statement which model better represents the aerodynamic dataset in this range is difficult to make.

In order to better assess the goodness of fit of both models, the Root Mean Squared Error (RMSE) and the Median Absolute Deviation (MAD) have been calculated between the posterior predictive distributions and each aerodynamic dataset. These results are presented in figure 9 and 10 for the high-fidelity datasets. Whereas the RMSE is one of the most common error metrics in statistics, the MAD metric is similar but less sensitive to outliers. It can be observed that the Reference Model has a smaller error to the TMK dataset than the Bayesian Model, in terms of both RMSE and MAD. Regarding the error to the HST dataset, the Reference Model seems to have a lower MAD, whereas the Bayesian Model might have a slightly lower RMSE. The RMSE of the Reference Model with respect to the TAU HF dataset is however higher than for the Bayesian Model, while both MADs are almost comparable.

Considering these error metrics, it could be concluded that the Reference Model slightly better fits the TMK dataset than the Bayesian Model. For all other measures the observed differences between the models are however not so significant, which can be also be seen by the wide overlap of their HDIs. Therefore, it can at least be concluded that the Bayesian Model and the Reference Model fit the aerodynamic datasets with roughly comparable quality. Furthermore, it can be observed that the spread of each error metric is lower for the Reference Model than for the Bayesian model. This basically supports the hypothesis that the deviations of the Reference Model are mostly caused by its bias, whereas the deviations of the Bayesian Model are more caused by its variance. It should be noted, that a smaller uncertainty spread does not indicate a better model. For the users of the AEDB underestimation of the uncertainties can lead to other subsystems not being designed robust enough, while an overestimation can lead to effort being spent to achieve a level of robustness not actually necessary for the mission. While both approaches include prior knowledge in the assessment of the uncertainties, the classical approach relies more on expert judgement, than the more data-driven Bayesian approach. Since such a vehicle has not been flown in Europe, the transfer of expert judgement from other aerodynamics configurations, has to be done with care. One of the goals of the CALLISTO project is

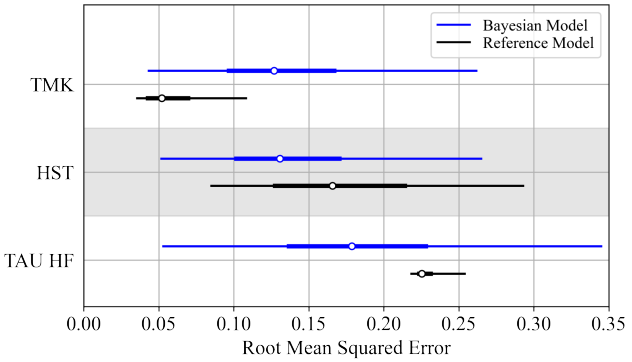


**Figure 9**. Forest plot of RMSE between posterior predictive distributions and different aerodynamic datasets for each model. Each bar indicates the mean value, the interquartile range and the 95% HDI.

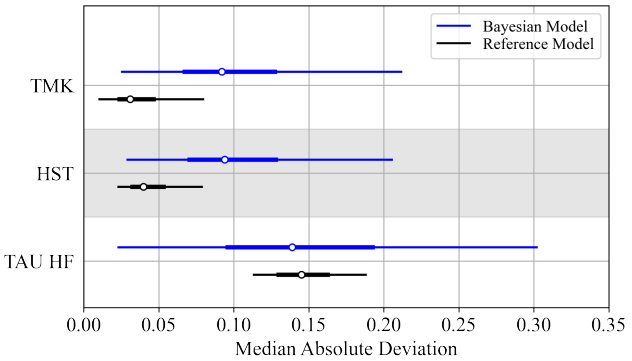


**Figure 10**. Forest plot of MAD between posterior predictive distributions and different aerodynamic datasets for each model. Each bar indicates the mean value, the interquartile range and the 95% HDI.

the generation of experience with this specific type of vehicle, which might lead to changed judgement of the uncertainty after the flights have been evaluated.

In summary, it can be concluded that although both models show slightly different characteristics, they have both the capabilities to adequately predict aerodynamic coefficient for unknown flight conditions with roughly comparable quality.

## 6. Conclusions and Outlook

In the scope of this paper the methodology to apply Bayesian Inference for the predictions of aerodynamic coefficients for unknown flight conditions has been developed. It could be shown that a Bayesian model for the generalized AEDB generation problem can be constructed. For CALLISTO this has been exemplified by a simple Gaussian Process model for the AoA dependency of the normal force coefficient. A software implementation of this model has be provided, which is able to automatically infer its parameters from the available aerodynamic datasets, and which is able to provide reasonable predictions of aerodynamic coefficients for new flight conditions, including quantified uncertainties. This demonstration showed already that the Bayesian approach is a noteworthy alternative to the classical AEDB generation.

For the implemented Bayesian model some first inference and predictions results have been presented and compared with the reference AEDB model of CALLISTO. It could be shown that all CFD and WTT results are covered well within the estimated uncertainties of the model. In direct comparison with the reference model, a larger variance has been observed in the predicted coefficients. However, the relatively low variance of the reference model is realized at the expense of a larger bias: Several aerodynamic datapoints are not covered by the estimated uncertainties of the reference model. Whether a higher variance or a higher bias is preferable for the AEDB model is a clear trade-off which needs further discussion with AEDB users and aerodynamic experts. Therefore, a clear statement which of both models better represents the uncertain aerodynamic behavior of the vehicle is not yet possible.

Furthermore, the fitting qualities for the predictive results of both models have been evaluated with different error metrics. Depending on the selected metric and the aerodynamic subset used for evaluation, one or the other model has shown slightly better results. However, significantly better performance could not be shown for any model. It can therefore at least be concluded, that the fitting qualities of both models are comparable.

Even though these observations are supporting the suitability of Bayesian Inference for the AEDB generation process, this study should only be interpreted as a first demonstration of this approach. As only one simple Bayesian model has been presented and examined in this paper, further tests would be necessary to generalize the results. Models for other aspects of CALLISTO's AEDB have already been tested by the authors, but not yet assessed to the presented degree of detail. Furthermore, the applicability of this approach should also be validated for other aerospace vehicles. At least for CALLISTO it is intended to prepare a full Bayesian characterization of the vehicle aerodynamic for an upcoming publication.

Finally, it should be noted that the presented Bayesian approach is not limited to the prediction of aerodynamic uncertainties only. These principles can also be applied to other field of engineering, where estimates with quantified uncertainties are required. Possible use cases are for example the vehicle mass estimation or the estimation of operational costs. Since Bayesian inference is not so common yet in engineering, the main difficultly is here the translation of classical approaches into suitable Bayesian models.

## Acknowledgments

The authors thank CNES and JAXA for the exemplary cooperation in the CALLISTO project. Without our joint effort this project would have not been possible.

## References

[1] S. Ishimoto, P. Tatiossian, and E. Dumont, "Overview of the callisto project," in *32nd International Symposium on Space Technology and Science (ISTS)*, 2019. [Online]. Available: https://archive.ists.or.jp/upload_pdf/2019-o-1-05.pdf

[2] E. Dumont, S. Ishimoto, P. Tatiossian, J. Klevanski, B. Reimann, T. Ecker, L. Witte, J. Riehmer, M. Sagliano, S. G. Vincenzino *et al.*, "Callisto: a demonstrator for reusable launcher key technologies," *Transactions of the Japan Society for Aeronautical and Space Sciences, Aerospace Technology Japan*, vol. 19, no. 1, pp. 106–115, 2021. [Online]. Available: https://www.jstage.jst.go.jp/article/tastj/19/1/19_19.106/_article

[3] J. Desmariaux, E. Cliquet Moreno, C. Chavagnac, P. Tatiossian, Y. Saito, and E. Dumont, "Callisto reusable vehicle system design," in *32nd International Symposium on Space Technology and Science (ISTS)*, 2019. [Online]. Available: https://archive.ists.or.jp/upload_pdf/2019-g-02.pdf

[4] DLR. (2020, Oct) Callisto. [Online]. Available: https://youtu.be/wAJ6cwDEme8

[5] L. E. Briese, T. M. Kier, I. Petkov, J. Windelberg, L. Heinrich, and S. Krummen, "Advanced modeling and dynamic stability analysis of the aerodynamic control surfaces of callisto," in *AIAA Scitech 2022 Forum*, 2022.

[6] S. Giagkozoglou Vincenzino, S. Eichel, W. Rotärmel, F. Krziwanie, I. Petkov, E. Dumont, A. Schneider, S. Schröder, J. Windelberg, T. Ecker *et al.*, "Development of reusable structures and mechanisms for callisto," in *33rd International Symposium on Space Technology and Science (ISTS)*, 2022. [Online]. Available: https://archive.ists.or.jp/upload_pdf/G-3-04.pdf

[7] S. Guédron, S. Ishimoto, E. Dumont, P. Tatiossian, C. Chavagnac, J. Desmariaux, D. Monchaux, O. Frenoy, E. C. Moreno, C. Deremaux, N. Lidon, N. Cesco, L. Witte, M. Sagliano, D. Seelbinder, J. Klevanski, T. Ecker, B. Reimann, J. Riehmer, M. Ertl, and S. Krummen, "Callisto demonstrator: Focus on system aspects," in *71th International Astronautical Congress*, Oktober 2020. [Online]. Available: https://elib.dlr.de/138808/

[8] M. Illig, S. Ishimoto, and E. Dumont, "Callisto, a demonstrator for reusable launchers," in *9th European Conference for Aeronautics and Space Sciences (EUCASS)*, Juni 2022. [Online]. Available: https://elib.dlr.de/187028/

[9] S. Ishimoto, M. Illig, and E. Dumont, "Development status of callisto," in *33rd International Symposium on Space Technology and Science (ISTS)*, 2022. [Online]. Available: https://archive.ists.or.jp/upload_pdf/G-3-02.pdf

[10] E. Dumont, S. Ishimoto, M. Illig, M. Sagliano, M. Solari, T. Ecker, H. Martens, S. Krummen, J. Desmariaux, Y. Saito *et al.*, "Callisto: towards reusability of a rocket stage: current status," in *33rd International Symposium on Space Technology and Science (ISTS)*, 2022. [Online]. Available: https://archive.ists.or.jp/upload_pdf/G-3-03.pdf

[11] S. Krummen, J. Desmariaux, Y. Saito, M. Boldt, L. E. Briese, N. Cesco, C. Chavagnac, E. Cliquet-Moreno, E. Dumont, T. Ecker, S. Eichel, M. Ertl, S. Giagkozoglou, T. Glaser, C. Grimm, M. Illig, S. Ishimoto, J. Klevanski, N. Lidon, O. Mierheim, J.-F. Niccolai, S. Reershemius, B. Reimann, J. Riehmer, M. Sagliano, H. Scheufler, A. Schneider, S. Schröder, R. Schwarz, D. Seelbinder, M. Stief, J. Windelberg, and S. Woicke, "Towards a reusable first stage demonstrator: Callisto - technical progresses & challenges," in *Proceedings of the International Astronautical Congress, IAC*, October 2021. [Online]. Available: https://elib.dlr.de/147143/

[12] E. Dumont, M. Illig, S. Ishimoto, C. Chavagnac, Y. Saito, S. Krummen, S. Eichel, H. Martens, S. Giagkozoglou, J. S. Häseker, T. Ecker, J. Klevanski, F. Krziwanie, W. Rotärmel, S. Schröder, A. Schneider, C. Grimm, S. Woicke, M. Sagliano, M. Schlotterer, M. Markgraf, B. Braun, M. Aicher, L. E. Briese, I. Petkov, J. Riehmer, and B. Reimann, "Callisto: A prototype paving the way for reusable launch vehicles in europe and japan," in *73rd International Astronautical Congress (IAC)*, September 2022. [Online]. Available: https://elib.dlr.de/188663/

[13] J. Klevanski, B. Reimann, S. Krummen, M. Ertl, T. Ecker, J. Riehmer, and E. Dumont, "Progress in aerodynamic studies for callisto - reusable vtvl launcher first stage demonstrator," in *9th European Conference for Aeronautics and Aerospace Sciences (EUCASS)*, June 2022. [Online]. Available: https://elib.dlr.de/187069/

[14] K. Hanemann, J. M. Schramm, A. Wagner, S. Karl, and V. Hanemann, "A closely coupled experimental and numerical approach for hypersonic and high enthalpy flow investigations utilising the heg shock tunnel and the dlr tau code," DLR, Tech. Rep., 2010.

[15] B. Thornber, A. Mosedale, D. Drikakis, D. Youngs, and R. Williams, "An improved reconstruction method for compressible flows with low mach number features," *Journal of Computational Physics*, vol. 227, no. 10, pp. 4873–4894, 2008. [Online]. Available: https://www.sciencedirect.com/science/article/pii/S0021999108000429

[16] P. Spalart and S. Allmaras, *A one-equation turbulence model for aerodynamic flows*, 1994. [Online]. Available: https://arc.aiaa.org/doi/abs/10.2514/6.1992-439

[17] M. Ertl, T. Ecker, J. Klevanski, S. Krummen, and E. Dumont, "Aerothermal analysis of plume interaction with deployed landing legs of the callisto vehicle," in *9th European Conference for Aeronautics and Space Sciences*, 2022.

[18] T. Ecker, M. Ertl, J. Klevanski, E. Dumont, and S. Krummen, "Aerothermal characterization of the callisto vehicle during descent," in *9th European Conference for Aeronautics and Space Sciences*, 2022.

[19] H. Versteeg and W. Malalasekera, *An Introduction to Computational Fluid Dynamics: The Finite Volume Method*. Pearson Education Limited, 2007. [Online]. Available: https://books.google.de/books?id=RvBZ-UMpGzIC

[20] I. B. Celik, U. Ghia, P. J. Roach, C. J. Freitas, H. Coleman, and P. E. Raad, "Procedure for estimation and reporting of uncertainty due to discretization in cdf application," *Journal of Fluids Engineering - Transactions of the ASME*, vol. 130, no. 7, 2008.

[21] T. Ecker, S. Karl, E. Dumont, S. Stappert, and D. Krause, "Numerical study on the thermal loads during a supersonic rocket retropropulsion maneuver," *Journal of Spacecraft and Rockets*, vol. 57, no. 1, pp. 131–146, 2020. [Online]. Available: https://doi.org/10.2514/1.A34486

[22] J. Riehmer, K. Kapteijn, J. Klevanski, B. Reimann, S. Krummen, A. Gülhan, and E. Dumont, "Wind tunnel experiments of the callisto vtvl launcher in the tmk

and hst wind tunnels," in *9th European Conference for Aeronautics and Space Sciences*, 2022.

[23] S. Krummen and M. Sippel, "Effects of the rotational vehicle dynamics on the ascent flight trajectory of the spaceliner concept," *CEAS Space Journal*, vol. 11, no. 2, pp. 161–172, 2019.

[24] C. Rosema, J. Doyle, L. Auman, M. Underwood, and W. B. Blake, "Missile datcom user's manual - 2011 revision," U.S. Army Aviation and Missile Research, Development and Engineering Center, Tech. Rep., 2011.

[25] J. Salvatier, T. V. Wiecki, and C. Fonnesbeck, "Probabilistic programming in python using pymc3," *PeerJ Computer Science*, vol. 2, p. e55, 2016.

[26] T. Wiecki, J. Salvatier, R. Vieira, M. Kochurov, A. Patil, B. Engels, J. Lao, M. Osthege, C. Carroll, O. A. Martin, B. T. Willard, A. Seyboldt, A. Rochford, rpgoldman, L. Paz, K. Meyer, P. Coyle, M. E. Gorelli, R. Kumar, O. Abril-Pla, T. Yoshioka, G. Ho, T. Kluyver, K. Beauchamp, A. Andorra, D. Pananos, E. Spaak, V. Andreani, B. Edwards, and E. Ma, "pymc-devs/pymc: v4.2.1," 9 2022. [Online]. Available: https://doi.org/10.5281/zenodo.7129432

[27] C. K. Williams and C. E. Rasmussen, *Gaussian processes for machine learning*. MIT press Cambridge, MA, 2006, vol. 2, no. 3.

[28] D. Duvenaud, "Automatic model construction with gaussian processes," Ph.D. dissertation, University of Cambridge, 2014.

[29] D. J. MacKay *et al.*, "Introduction to gaussian processes," *NATO ASI series F computer and systems sciences*, vol. 168, pp. 133–166, 1998.

[30] Space Systems Group, "Aerodynamic design data book orbiter vehicle sts-1," Rockwell International, Tech. Rep., 1980.

[31] J. Weil and P. B. G, "Correlation of predicted and flight derived stability and control derivatives with particular application to tailless delta wing configurations," NASA, Tech. Rep. NASA TM-81361, 1981.

[32] V. Wartemann, N. Konosidou, A. Flock, and C. Merrem, "Contribution of numerical and experimental flow simulations to the aerodynamic data base of the dlr reusable flight experiment refex," in *Notes on Numerical Fluid Mechanics and Multidisciplinary Design*, vol. 151. Springer, 2020.

[33] A. Schettino, G. Pezzella, M. Marini, S. Di Benedetto, V. F. Villace, J. Steelant, R. Choudhury, A. Gubanov, and N. Voevodenko, "Aerodynamic database of the hexafly-int hypersonic glider," *CEAS Space Journal*, vol. 12, no. 2, 2022.

[34] P. Roncioni, P. L. Vitagliano, F. De Gregorio, F. Paglia, and C. Milana, "Aerodatabase of vega-c launcher development and integration," in *Proceedings of 8th European Conference for Aeronautics and Space Sciences, Madrid, Spain*, 2019. [Online]. Available: https://www.eucass.eu/doi/EUCASS2019-0130.pdf

[35] M. Stradtner, C. M. Liersch, and P. Bekemeyer, "An aerodynamic variable-fidelity modelling framework for a low-observable ucav," *Aerospace Science and Technology*, vol. 107, p. 106232, 2020.

[36] S. A. Renganathan, K. Harada, and D. N. Mavris, "Aerodynamic data fusion toward the digital twin paradigm," *AIAA Journal*, vol. 58, no. 9, pp. 3902–3918, 2020.

[37] R. Hall, S. Holland, and J. Blevins, "Aerodynamic characterization of a modern launch vehicle," in *49th AIAA Aerospace Sciences Meeting including the New Horizons Forum and Aerospace Exposition*, 2011, p. 10.

[38] J. G. Hoffer, B. C. Geiger, and R. Kern, "Gaussian process surrogates for modeling uncertainties in a use case of forging superalloys," *Applied Sciences*, vol. 12, no. 3, p. 1089, 2022.

[39] Y. Morita, S. Rezaeiravesh, N. Tabatabaei, R. Vinuesa, K. Fukagata, and P. Schlatter, "Applying bayesian optimization with gaussian process regression to computational fluid dynamics problems," *Journal of Computational Physics*, vol. 449, p. 110788, 2022.

[40] Y. Li, S. Rao, A. Hassaine, R. Ramakrishnan, D. Canoy, G. Salimi-Khorshidi, M. Mamouei, T. Lukasiewicz, and K. Rahimi, "Deep bayesian gaussian processes for uncertainty estimation in electronic health records," *Scientific reports*, vol. 11, no. 1, pp. 1–13, 2021.

[41] Y. Zhao, F. Yin, F. Gunnarsson, and F. Hultkrantz, "Gaussian processes for analyzing positioned trajectories in sports," *arXiv preprint arXiv:1907.03043*, 2019.

[42] Stan Development Team, *Stan User's Guide*, Feb 2022. [Online]. Available: https://mc-stan.org/docs/2_29/stan-users-guide-2_29.pdf

[43] A. Gelman, A. Vehtari, A. Riddell, B. Bales, P. Wilson, M. Lawrence, and M. Betancourt. (2020, Apr) Prior choice recommendations. Stan Development Team. [Online]. Available: https://github.com/stan-dev/stan/wiki/Prior-Choice-Recommendations

[44] U. Von Luxburg and B. Schölkopf, "Statistical learning theory: Models, concepts, and results," in *Handbook of the History of Logic*. Elsevier, 2011, vol. 10, pp. 651–706.